

Synthesis and characterization of polymeric hydrogel-based nanoporous composite and investigation of its temperature-dependent drug release activity

Akhilesh Kumar Maurya, Shagun Varshney, Nidhi Mishra✉

Department of Applied Sciences, Indian Institute of Information Technology, Allahabad, Prayagraj, Uttar Pradesh, 211012, India

✉ nidhimishra@iiita.ac.in

Abstract. Hydrogels are 3-dimensional polymeric networks that undergo swelling when placed in an aqueous medium. The hydrogel-based polymers can respond to changes in the surrounding like temperature, pressure, pH, etc. Widespread cross-linking in hydrogels provides it with robustness, propensity for water, and better mechanical properties. The present work reports the one-pot chemical synthesis of a co-polymeric hydrogel-based composite using 2-HEMA (hydroxyethyl methacrylate), PEGMA (Polyethylene glycol), and PNIPAM (Poly (N-isopropyl acrylamide)). Extensive water retention ability and biocompatibility are some distinguishing features that enable it to be used for various biomedical applications. The hydrogel was characterized using X-ray diffraction analysis for its crystalline nature, scanning electron microscopy for surface morphology and pore size, and Fourier transform infrared spectroscopy for functional group analysis. Drug loading and release activity was performed and analyzed by Ultraviolet-Visible spectroscopy.

Keywords: composite, characterization, drug loading, hydrogel, thermos-responsive polymer

Acknowledgements. *The authors thank the Indian Institute of Information Technology, Allahabad, and BBAU, Lucknow, for providing the material characterization facilities. The authors also acknowledge UPCST for financial assistance.*

Citation: Akhilesh Kumar Maurya, Shagun Varshney, Nidhi Mishra. Synthesis and characterization of polymeric hydrogel-based nanoporous composite and investigation of its temperature-dependent drug release activity. *Materials Physics and Mechanics*. 2022;50(2): 275-286. DOI: 10.18149/MPM.5022022_8.

1. Introduction

Hydrogels are a network of polymer(s) that can absorb water and still can remain insoluble in water. They show swelling behavior after imbibing water in their pores [1-4]. Permeability and water retention properties are the characteristic features of such hydrogels. They undergo hydration due to the presence of hydrophilic groups and are also observed to exhibit viscoelastic properties [5]. The extensive cross-linking between the groups makes them insoluble and gives them a robust structure and enhanced mechanical properties [6-8]. The cross-linking may be due to the chemical and or physical interaction between the covalent bonds. The water retention properties of hydrogels make them excellent biocompatible agents [9,10], where their hydrophilic, rubber-like nature causes negligible tissue irritation. It also

© Akhilesh Kumar Maurya, Shagun Varshney, Nidhi Mishra, 2022.

Publisher: Peter the Great St. Petersburg Polytechnic University

This is an open access article under the CC BY-NC 4.0 license (<https://creativecommons.org/licenses/by-nc/4.0/>)

prevents them from adhering to the surface of cells and proteins [11,12]. Hydrogels may be chemically stable or degrade depending on the chemical composition and cross-linking extent [13]. Natural polymers such as gelatin, chitosan, agar, etc., and synthetic polymers like polyacrylamide, methacrylate esters, etc., can prepare such hydrogels. They can be synthesized using polymer-polymer cross-linking, copolymerization, and reactive precursors [14-17]. Hydrogels can be classified as homopolymer (single monomer), copolymer (more than one monomer), and multi-polymer (more than one polymer) [18-20].

Hydrogels are responsive to stimuli like pressure, pH, reagent concentration, and temperature [21-23]. The behavior of polymers adapting to structural changes in response to physical or chemical stimuli makes them suitable for synthesizing smart polymers. Thermo-responsive and pH-sensitive polymeric hydrogels are one of the essential identities being used for several applications [24-27]. Thermo-responsive polymers belong to the class of smart polymers that respond to temperature changes. This makes them readily available for controlled drug delivery and other medical applications. Thermo-responsive polymers may either collapse or expand around their critical temperature. PNIPAM (Poly (N- isopropyl acrylamide)) is a thermo-responsive polymer that has been used for drug delivery for decades [28-30]. It transitions from hydration to dehydration at a lower critical solution temperature (LCST) of 32°C. Below the LCST, PNIPAM exists in a fully swollen state, but above the LCST, it shrinks [31-34].

HEMA (Poly-hydroxy-ethyl-methacrylate) is a hydrophilic and stable polymer formed from the monomer hydroxyethyl methacrylate. It has received considerable recognition for years owing to its simple synthesis and applications in biomedical engineering [35-38]. PEGMA (Polyethylene glycol) does not initiate an immune response and even does not adhere to proteins in the body [39]. Although hydrophobic, it becomes hydrophilic and swells up by water absorption by side groups. This polymer has been reported to have excellent biocompatibility and properties similar to living tissues [40-42]. It also has a hydroxyl functional group that can be utilized for protein conjugation. The conjugation of PNIPAM is done with methacrylate to enhance the mechanical property of the hydrogels [43-46]. Hydrogels have been used in medical applications [47-50], which include the preparation of contact lenses [51,52], tissue engineering [53,54], drug delivery [55-57], etc.

In the present study, one-pot synthesis of hydrogel-based polymeric composite has been carried out using 2-HEMA, PEGMA, and PNIPAM as the starting precursors. The synthesis and characterization of the hydrogel are also accompanied by the investigation of the drug release activity of curcumin observed in the simulated body fluid (SBF). Several characterization techniques, including X-ray diffraction (XRD), Scanning Electron Microscopy (SEM), Fourier transform infrared spectroscopy (FTIR), and Ultraviolet-Visible (UV-Vis) Spectroscopy, have been used to analyze the structural, morphological, and physio-chemical characteristics of the synthesized composite.

2. Material and methods

For the synthesis of hydrogel, the chemical reagents required were 2-HEMA (2-Hydroxy-methacrylate, 99% assay), NIPAM (N-Isopropylacrylamide, 99% assay), PEGMA (poly (ethylene glycol) methacrylate, 99.5% assay), APS (Ammonium persulfate, 99% assay), MBA (N, N'-Methylene Bis(acrylamide), 99% assay), and nitrogen gas. For the preparation of simulated body fluid, NaCl (Sodium chloride, 99% assay), NaHCO₃ (Sodium bicarbonate, 99.5% assay), KCl (Potassium chloride, 99% assay), Na₂HPO₄ (Sodium phosphate, 99% assay), MgCl₂.6H₂O (Magnesium chloride hexahydrate, 99% assay), HCl (hydrochloric acid, 99% assay), CaCl₂.2H₂O (Calcium chloride dehydrate, 99% assay), Na₂SO₄ (Sodium sulfate, 99.5% assay), TRIS tris(hydroxymethyl)aminomethane (99.5% assay), and Curcumin (99.5% assay) were used for investigating the drug release activity. All chemicals used were of

analytical grade and were purchased from Merck. & Co. Double-distilled water was used throughout the experiment.

Synthesis of hydrogel-based polymeric composite. NIPAM (1.13 g), 2-HEMA (1.2 mL), and PEGMA (3.26 mL) were mixed in a round bottom flask under continuous stirring. After some time, 1% APS solution (60 μ L) was added as an indicator for reaction, and 5% of MBA (280 μ L) was added as a cross-linking agent. The flask was sealed under the continuous flow of nitrogen gas (to provide an inert atmosphere for reaction). Flask was then transferred to the water bath at 80 °C for 3.5 h. to promote the polymerization reaction. After synthesis, the hydrogel was placed in deionized water for three days, and the water was periodically replaced with fresh double-distilled water. The experimental setup for the synthesis of hydrogel is shown in Fig. 1.

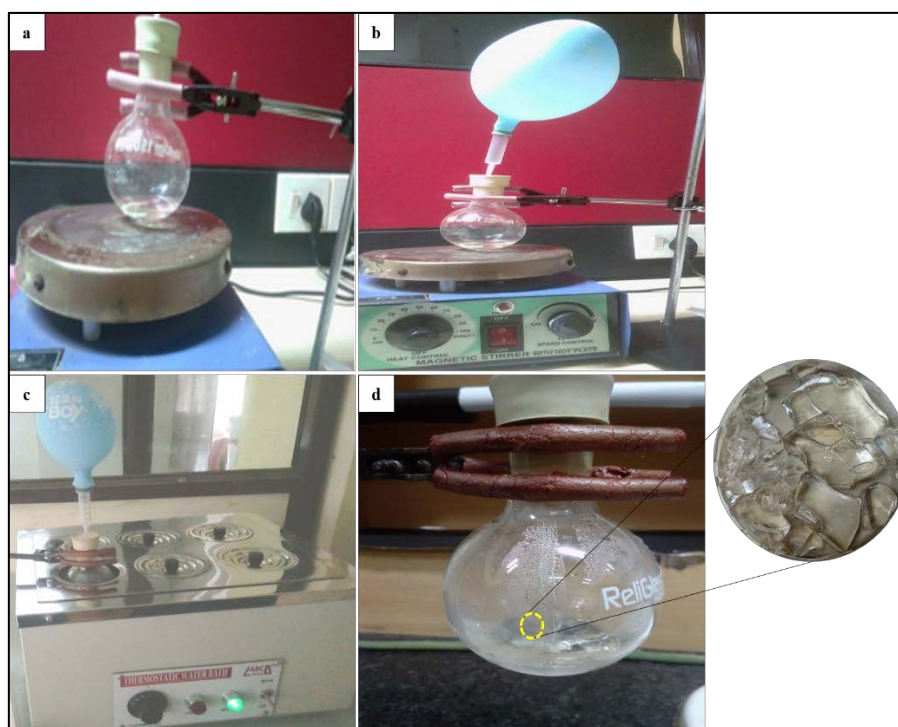


Fig. 1. (a), (b), (c), and (d) Laboratory synthesis of polymeric hydrogel

Preparation of simulated body fluid. NaCl (3.3 g), NaHCO₃ (1.1 g), KCl (0.19 g), Na₂HPO₄ (0.09 g), and MgCl₂·6H₂O (0.15 g) were added to a flask, and mixed, thoroughly in 350 mL of double distilled water. After that, 7.5 mL of HCl was added to the above mixture, followed by the addition of CaCl₂·2H₂O (0.18 g), Na₂SO₄ (0.04 g), and TRIS (3.03 g). HCl (12.5 mL) was added to maintain the desired pH of SBF. The flowchart for the synthesis of SBF is shown in Fig. 2.

Drug loading and release analysis. Curcumin (100 mg) was dissolved in 5 mL of acetone solution, and 20 mg of synthesized hydrogel was added to the solution and kept for 24 h. to load the curcumin into the hydrogel. The percentage of drug-loaded was evaluated by taking the weight of the loaded hydrogel. The flowchart for loading drugs into the hydrogel composite is shown in Fig. 3.

The drug-hydrogel complex was placed in 20 mL of SBF for 30 min under continuous stirring for a definite time interval. After that, the absorption of SBF was analyzed by UV-Vis spectroscopy. The mixture temperature was increased by 10 °C for the next reading. Further, the temperature was raised by 5 °C up to 50 °C, and the readings were again recorded. The experimental setup for loading the drug is shown in Fig. 4.

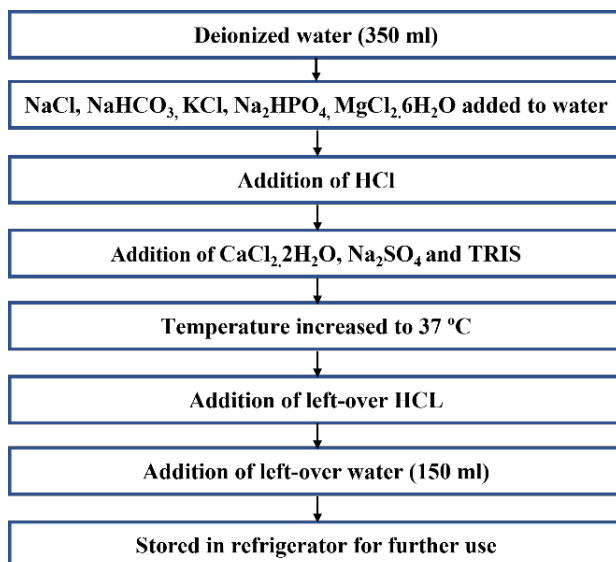


Fig. 2. Flowchart for the synthesis of simulated body fluid

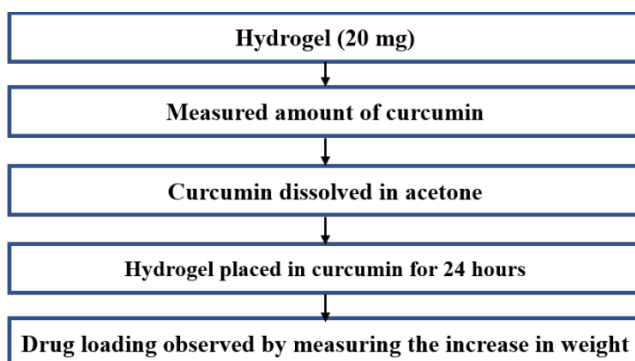


Fig. 3. Flowchart for drug loading and release analysis

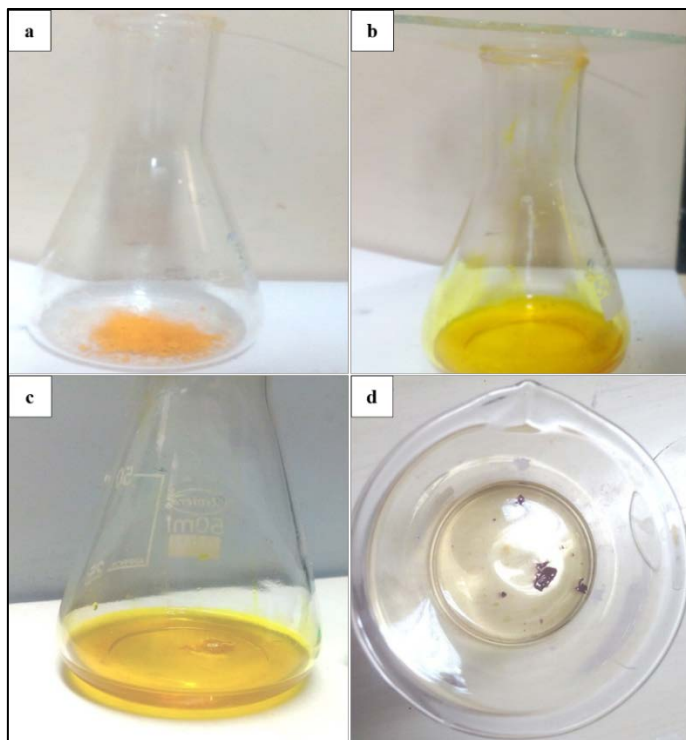


Fig. 4. Experimental setup for the loading of drug

3. Results and discussion

X-Ray diffraction analysis. The most frequent type of XRD used to examine solid-state materials is powder diffraction, which may accept samples in powder, thin film, or even in bulk form. Most investigations on supramolecular hydrogels have concentrated on this feature of XRD, which is an excellent technique for aiding in the analysis of crystalline materials in general [58]. It is worth noting that there are other varieties of XRD, including wide-angle X-ray diffraction and small-angle X-ray scattering, which are being increasingly utilized to analyze the structure of biological macromolecules, including hydrogels [59]. XRD analysis was performed to investigate the crystalline and structural characteristics of the hydrogel composite (Model: Rigaku Miniflex 600 Desktop X-Ray Diffraction System). The diffraction pattern of the hydrogel composite is shown in Fig. 5. The intensity of diffraction for the samples was recorded at a wavelength of 1.541 Å with a diffraction angle (2θ) ranging from 0° to 80° with a scanning rate of 5°/min. A pure sample of synthesized hydrogel does not exhibit any sharp peaks, as shown in the diffraction patterns. The absence of sharp crystalline peaks reveals the amorphous nature of the synthesized composite. A single broad peak at a $2\theta = 20^\circ$ angle attributes to the synthesized hydrogel polymeric network, which is in accordance with Varaprasad *et al.* [60].

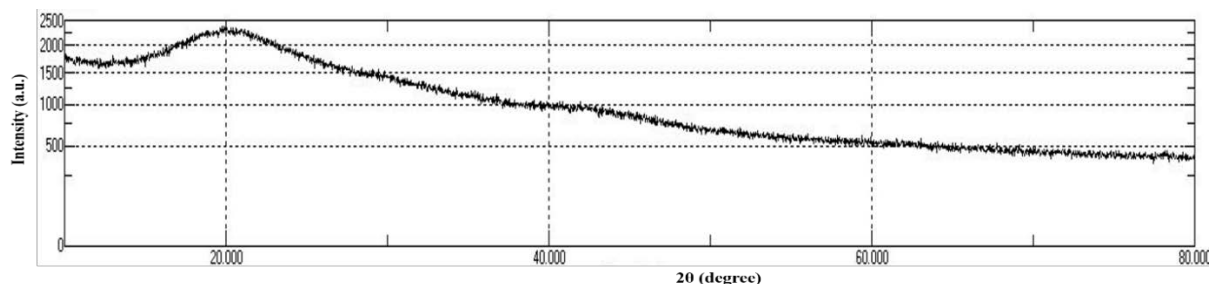


Fig. 5. Diffraction patterns for the synthesized hydrogel composite

Scanning electron microscopy analysis. Electron microscopes use a stream of electrons to provide high-resolution pictures of materials. However, the analyte might be damaged as a result. To eliminate beam interference, a vacuum is required, which implies samples must be dried before imaging. Although it is less detailed and only gives surface imaging of materials, the method does not need considerable sample preparation for frequent usage. While SEM offers information about the surface of hydrogel, focused ion beam -SEM can be employed for obtaining a 3D image for the same. The surface morphology and pore size of the hydrogel composite were analyzed by SEM (Model: JSM-6490LV, JEOL, JAPAN). The surface morphology of hydrogel depicted the compactness of structure and arrangement of monomers for polymer synthesis. As seen in Figures 6, (a), (b), (c), and (d), porous structure with rough surface morphology can be observed. The hydrogel was observed to have well cross-linked monomers to form a polymeric network. At a much higher magnification, pore size with an average diameter between 23-104 nm for the synthesized hydrogel can be observed in Fig. 6 (d). The pores allow water, drug, and other molecules to be absorbed in the swollen state. When dried, water molecules get evaporated, and the entrapment of the drug takes place in the hydrogel.

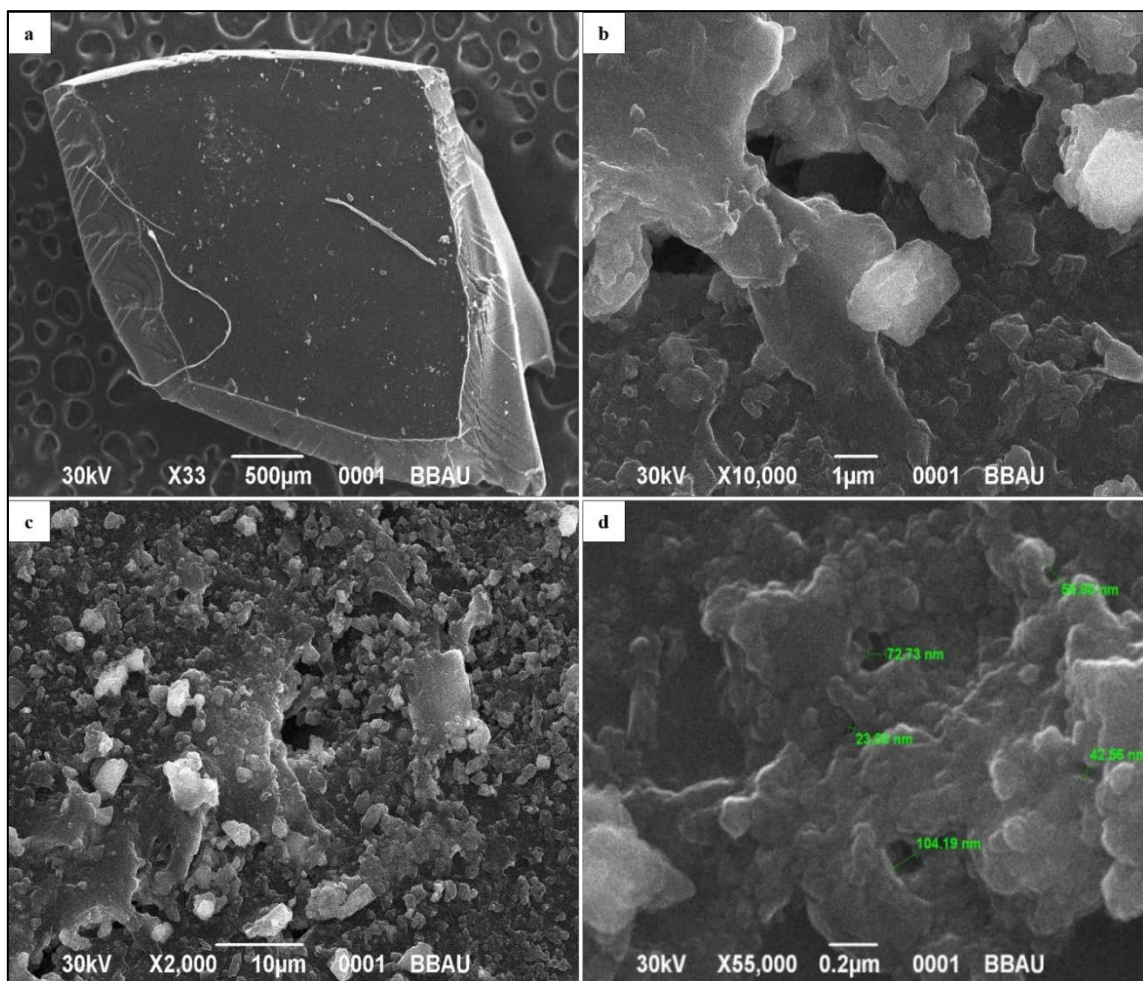


Fig. 6. Scanning electron micrographs for morphological analysis of the synthesized hydrogel

Fourier transform infrared spectroscopy analysis. Although it uses infrared light, FTIR spectroscopy works similarly to UV–vis spectroscopy. FTIR infers the absorbance spectrum precisely by applying the Fourier transform process to absorbance measurements of numerous wavelengths of light at the same time. Certain stretching vibrations on FTIR spectra correlate to certain functional groups, allowing the approach to describe the atomic structure of the hydrogel or solution or establish its composition in other ways [61]. FTIR spectroscopy (Model: NicoletTM6700, Thermo Scientific, USA) in attenuated total reflection mode in the range from 4000 to 500 cm^{-1} with 4 cm^{-1} as the resolution. The FTIR spectrum reveals the different functional groups in the synthesized hydrogel composite. The FTIR spectrum exhibited different peaks at 3429.7 cm^{-1} , 2915.3 cm^{-1} , 1725.6 cm^{-1} , 1643.5 cm^{-1} , 1552.8 cm^{-1} , 1425.5 cm^{-1} , 1358.8 cm^{-1} , 1161.6 cm^{-1} , 1067.5 cm^{-1} and 605.1 cm^{-1} is shown in Fig. 7. The peak at 3429.7 cm^{-1} is a characteristic of the hydroxyl-based copolymer, indicating the presence of 2-HEMA. The peak at 2915.3 cm^{-1} is attributed to carboxylic acid in the monomers. The peak at 1725.6 cm^{-1} corresponds to the carbonyl group present in all monomers. The peak at 1643.5 cm^{-1} represents the stretching in alkenes (C=C). The peak at 1552.8 cm^{-1} indicates the stretching of C=C aromatic/conjugate units, revealing the presence of aromatic groups in the hydrogel. The peak at 1425.5 cm^{-1} depicts the stretching of alkane in the polymeric network. 1358.8 cm^{-1} indicates the presence of (C-N) stretch of PNIPAM. The peak value of 1161.6 cm^{-1} and 1067.5 cm^{-1} represents O-H groups present in PEGMA. The functional groups' monomers are attracted to each other and form polymeric networks with the pores, which can absorb/entrap the molecules and release them to the desired place.

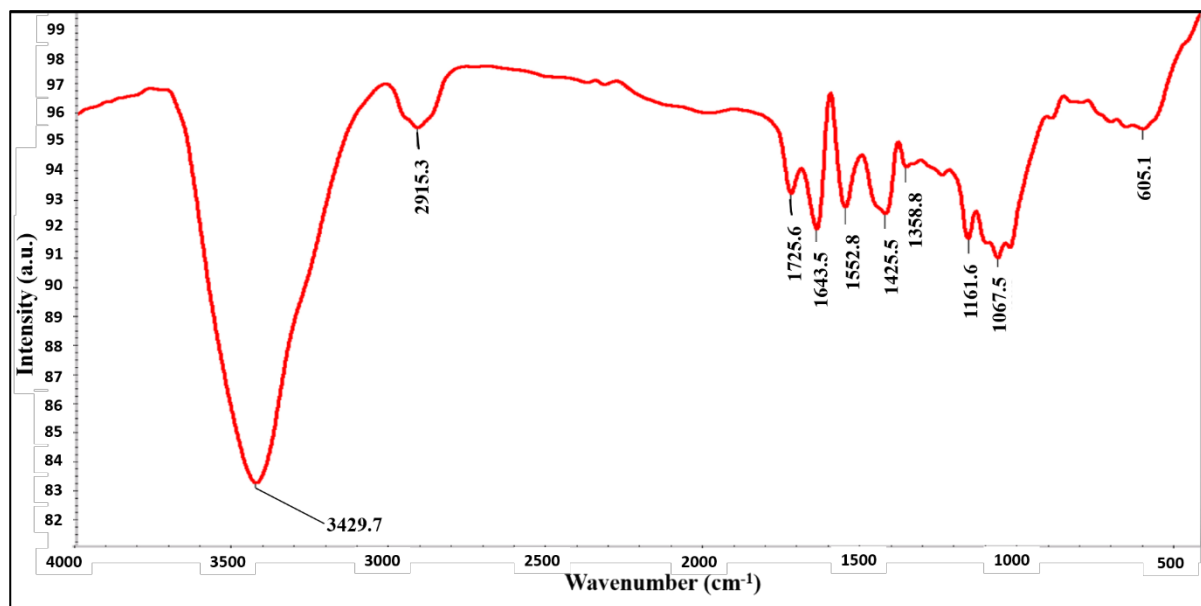


Fig. 7. Infrared spectrum for the analysis of functional groups in the synthesized hydrogel

Swelling behavior, drug loading, and drug release profile analysis. Swelling behavior studies were performed on the synthesized hydrogel composite. The dry weight of hydrogel was 20 mg; after incorporating water within its network, the weight increased to 50 mg. Thus, using the formula for calculating the swelling percentage, the degree of swelling of the hydrogel sample was found to be 75%. After the polymerization reaction, the hydrogel was soaked in water, and a slow increase in the volume was observed. When the swollen hydrogel was dried in an oven at 50 °C, the polymeric network of hydrogel collapsed, releasing the retained water molecules, and a shrinking in size was observed. The dry weight of hydrogel was taken, which was observed to be 20 mg. Then after placing it in curcumin solution in acetone for 24 h, the weight increased to 32 mg. The percentage Loading efficiency is computed to be around 60% by using the formula below.

$$\text{Drug loading \%} = \frac{\text{HD} - \text{HO}}{\text{HO}} \times 100.$$

In the above equation, HO – weight of the dry hydrogel, HD – weight of the drug-loaded hydrogel. UV-Vis analysis for drug release is shown in Fig. 8, and the temperature-dependent drug release profile is shown in Fig. 9.

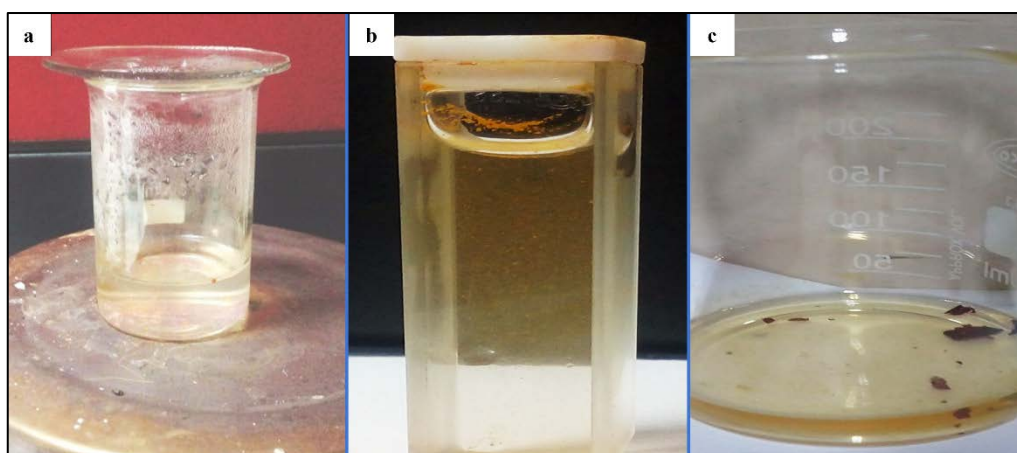


Fig. 8. Ultraviolet-Visible analysis for the release of drug by hydrogel composite

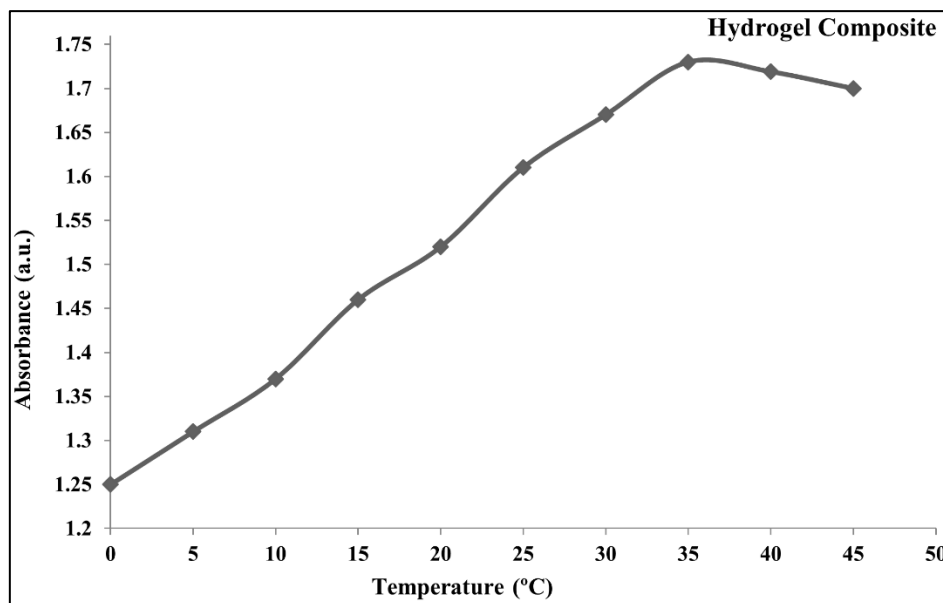


Fig. 9. Temperature-dependent drug release profile for hydrogel composite

The hydrogel was placed in SBF for releasing the drug and calculating its drug release percentage. Absorbance readings were taken at different temperatures. The hydrogel composite started to remove the drug as soon as it was placed in SBF. The absorbance value was observed to increase, indicating the release of curcumin slowly until the temperature reached 35 °C. Above 35 °C, absorbance reading almost became stagnant. Thus, the release percentage was computed and found to be around 26.47 %. Therefore, further studies can be carried out to optimize the efficacy of drug release. The release percentage was calculated by using the formula below:

$$\text{Release \%} = \frac{\text{Absorbance at final temperature} - \text{Absorbance at initial temperature}}{\text{Absorbance at final temperature}} \times 100.$$

4. Conclusions

Hydrogel composite was successfully synthesized using monomer of 2-HEMA, PEGMA, and NIPAM with pores lying within the nanometer range. Synthesized hydrogel responded to external stimuli like pH, temperature, etc. Hydrogels with cross-linked structures and amorphous nature were observed to have various functional groups. A study on the swelling behavior was also performed on the hydrogel by soaking it in an aqueous solution, and it exhibited a swelling percentage of 75%. Curcumin, an anti-cancer drug, was successfully loaded into the hydrogel, and the release characteristics were observed in SBF. Hydrogel composite showed sustained release of curcumin in SBF. Therefore, it can be further tailored to increase the loading and release efficiency of the drug. It can also be used for delivering therapeutic medications to targeted sites shortly.

References

1. Motamedi E, Motesharezedeh B, Shirinfekr A, Samar SM. Synthesis and swelling behavior of environmentally friendly starch-based superabsorbent hydrogels reinforced with natural char nano/micro particles. *Journal of Environmental Chemical Engineering*. 2020;8(1): 103583.
2. Shoukat H, Buksh K, Noreen S, Pervaiz F, Maqbool I. Hydrogels as potential drug-delivery systems: Network design and applications. *Therapeutic Delivery*. 2021;12(5): 375-396.

3. Ahmadi M, Zholobko O, Wu XF. Inhomogeneous swelling behavior of a bi-layered spherical hydrogel containing a hard core. *Journal of Applied Physics*. 2020;128(4): 044703.
4. Rehman TU, Bibi S, Khan M, Ali I, Shah LA, Khan A, Ateeq M. Fabrication of stable superabsorbent hydrogels for successful removal of crystal violet from waste water. *RSC Advances*. 2019;9(68): 40051-40061.
5. McKenzie M, Betts D, Suh A, Bui K, Kim LD, Cho H. Hydrogel-based drug delivery systems for poorly water-soluble drugs. *Molecules*. 2015;20(11): 20397-20408.
6. Kopecek J. Hydrogels: From soft contact lenses and implants to self-assembled nanomaterials. *Journal of Polymer Science Part A: Polymer Chemistry*. 2009;47(22): 5929-5946.
7. Bao Z, Xian C, Yuan Q, Liu G, Wu J. Natural polymer-based hydrogels with enhanced mechanical performances: preparation, structure, and property. *Advanced Healthcare Materials*. 2019;8(17): 1900670.
8. Ali A, Ahmed S. Recent advances in edible polymer based hydrogels as a sustainable alternative to conventional polymers. *Journal of Agricultural and Food Chemistry*. 2018;66(27): 6940-6967.
9. Zander ZK, Hua G, Wiener CG, Vogt BD, Becker ML. Control of Mesh Size and Modulus by Kinetically Dependent Cross-Linking in Hydrogels. *Advanced Materials*. 2015;27(40): 6283-6288.
10. Zhang D, Tang Y, Zhang Y, Yang F, Liu Y, Wang X, Yang J, Gong X, Zheng J. Highly stretchable, self-adhesive, biocompatible, conductive hydrogels as fully polymeric strain sensors. *Journal of Materials Chemistry A*. 2020;8(39): 20474-20485.
11. Kamath KR, Park K. Biodegradable hydrogels in drug delivery. *Advanced Drug Delivery Reviews*. 1993;11(1-2): 59-84.
12. Yu J, Wang K, Fan C, Zhao X, Gao J, Jing W, Zhang X, Li J, Li Y, Yang J, Liu W. An Ultrasoft Self-Fused Supramolecular Polymer Hydrogel for Completely Preventing Postoperative Tissue Adhesion. *Advanced Materials*. 2021;33(16): 2008395.
13. Hoare TR, Kohane DS. Hydrogels in drug delivery: Progress and challenges. *Polymer*. 2008;49(8): 1993-2007.
14. Elmehbad NY, Mohamed NA. Terephthalohydrazido cross-linked chitosan hydrogels: Synthesis, characterization and applications. *International Journal of Polymeric Materials and Polymeric Biomaterials*. 2022;71(13): 969-982.
15. Li S, Wang L, Yu X, Wang C, Wang Z. Synthesis and characterization of a novel double cross-linked hydrogel based on Diels-Alder click reaction and coordination bonding. *Materials Science and Engineering: C*. 2018;82: 299-309.
16. Elsayed MM. Hydrogel preparation technologies: relevance kinetics, thermodynamics and scaling up aspects. *Journal of Polymers and the Environment*. 2019;27(4): 871-891.
17. Zainal SH, Mohd NH, Suhaili N, Anuar FH, Lazim AM, Othaman R. Preparation of cellulose-based hydrogel: A review. *Journal of Materials Research and Technology*. 2021;10: 935-952.
18. Hua J, Ng PF, Fei B. High-strength hydrogels: Microstructure design, characterization and applications. *Inc. J. Polym. Sci., Part B: Polym. Phys.* 2018;56: 1325-1335.
19. Sharma S, Tiwari S. A review on biomacromolecular hydrogel classification and its applications. *International Journal of Biological Macromolecules*. 2020;162: 737-747.
20. Bashir S, Hina M, Iqbal J, Rajpar AH, Mujtaba MA, Alghamdi NA, Wageh S, Ramesh K, Ramesh S. Fundamental concepts of hydrogels: Synthesis, properties, and their applications. *Polymers*. 2020;12(11): 2702.
21. Deen GR, Loh XJ. Stimuli-responsive cationic hydrogels in drug delivery applications. *Gels*. 2018;4(1): 13.

22. Roy A, Manna K, Pal S. Recent advances in various stimuli-responsive hydrogels: from synthetic designs to emerging healthcare applications. *Materials Chemistry Frontiers*. 2022;6(17): 2338-2385
23. Lim WJ, Ooi BS. Applications of responsive hydrogel to enhance the water recovery via membrane distillation and forward osmosis: A review. *Journal of Water Process Engineering*. 2022;47: 102828.
24. Aswathy SH, Narendrakumar U, Manjubala I. Commercial hydrogels for biomedical applications. *Heliyon*. 2020;6(4): e03719.
25. Radvar E, Azevedo HS. Supramolecular peptide/polymer hybrid hydrogels for biomedical applications. *Macromolecular Bioscience*. 2019;19(1): 1800221.
26. Pasparakis G, Tsitsilianis C. LCST polymers: Thermoresponsive nanostructured assemblies towards bioapplications. *Polymer*. 2020;211: 123146.
27. Sarwan T, Kumar P, Choonara YE, Pillay V. Hybrid thermo-responsive polymer systems and their biomedical applications. *Frontiers in Materials*. 2020;7: 73.
28. Cao M, Wang Y, Hu X, Gong H, Li R, Cox H, Zhang J, Waigh TA, Xu H, Lu JR. Reversible thermoresponsive peptide–PNIPAM hydrogels for controlled drug delivery. *Biomacromolecules*. 2019;20(9): 3601-3610.
29. Doberenz F, Zeng K, Willems C, Zhang K, Groth T. Thermoresponsive polymers and their biomedical application in tissue engineering—a review. *Journal of Materials Chemistry B*. 2020;8(4): 607-628.
30. Xu X, Liu Y, Fu W, Yao M, Ding Z, Xuan J, Li D, Wang S, Xia Y, Cao M. Poly (N-isopropylacrylamide)-based thermoresponsive composite hydrogels for biomedical applications. *Polymers*. 2020;12(3): 580.
31. Chen Z, Chen Y, Chen C, Zheng X, Li H, Liu H. Dual-gradient PNIPAM-based hydrogel capable of rapid response and tunable actuation. *Chemical Engineering Journal*. 2021;424: 130562.
32. Tang L, Wang L, Yang X, Feng Y, Li Y, Feng W. Poly (N-isopropylacrylamide)-based smart hydrogels: Design, properties and applications. *Progress in Materials Science*. 2021;115: 100702.
33. Wang L, Liu F, Qian J, Wu Z, Xiao R. Multi-responsive PNIPAM–PEGDA hydrogel composite. *Soft Matter*. 2021;17(46): 10421-10427.
34. Harrer J, Rey M, Ciarella S, Löwen H, Janssen LM, Vogel N. Stimuli-responsive behavior of PNIPAm microgels under interfacial confinement. *Langmuir*. 2019;35(32): 10512-10521.
35. Singhal P, Vashisht H, Nisar S, Mehra S, Rattan S. Stimulus responsive soy-protein based hydrogels through grafting HEMA for biomedical applications. *Industrial Crops and Products*. 2022;178: 114621.
36. Yilmaz B, Ozay O. Synthesis, Characterization and Biomedical Applications of p (HEMA-co-APTMACI) Hydrogels Crosslinked with Modified Silica Nanoparticles. *Biointerface Res. Appl. Chem*. 2022;12: 3664-3680.
37. Gopanna A, Rajan KP, Thomas SP, Chavali M. Polyethylene and polypropylene matrix composites for biomedical applications. In: *Materials for Biomedical Engineering*. Elsevier; 2019. p.175-216.
38. Egbo MK. A fundamental review on composite materials and some of their applications in biomedical engineering. *Journal of King Saud University-Engineering Sciences*. 2021;33(8): 557-568.
39. Tarno H, Qi H, Endoh R, Kobayashi M, Goto H, Futai K. Types of frass produced by the ambrosia beetle *Platypus quercivorus* during gallery construction, and host suitability of five tree species for the beetle. *Journal of Forest Research*. 2011;16(1): 68-75.

40. Chen SL, Fu RH, Liao SF, Liu SP, Lin SZ, Wang YC. A PEG-based hydrogel for effective wound care management. *Cell Transplantation*. 2018;27(2): 275-284.
41. Shi J, Yu L, Ding J. PEG-based thermosensitive and biodegradable hydrogels. *Acta biomaterialia*. 2021;128: 42-59.
42. Han Y, Tang J, Liu S, Zhao X, Wang R, Xia J, Qin C, Chen H, Lin Q. Cellular microenvironment-sensitive drug eluting coating on intraocular lens for enhanced posterior capsular opacification prevention and in vivo biocompatibility. *ACS Applied Bio Materials*. 2020;3(6): 3582-3593.
43. Ross M, Hicks EA, Rambarran T, Sheardown H. Thermo-sensitivity and erosion of chitosan crosslinked poly [N-isopropylacrylamide-co-(acrylic acid)-co-(methyl methacrylate)] hydrogels for application to the inferior fornix. *Acta Biomaterialia*. 2022;141: 151-163.
44. Gao D, Duan L, Wu M, Wang X, Sun Z, Zhang Y, Li Y, He P. Preparation of thermo/redox/pH-stimulative poly (N-isopropylacrylamide-co-N, N'-dimethylaminoethyl methacrylate) nanogels and their DOX release behaviors. *Journal of Biomedical Materials Research Part A*. 2019;107(6): 1195-1203.
45. Mohammadi M, Arabi L, Alibolandi M. Doxorubicin-loaded composite nanogels for cancer treatment. *Journal of Controlled Release*. 2020;328: 171-191.
46. Ko CH, Henschel C, Meledam GP, Schroer MA, Müller-Buschbaum P, Laschewsky A, Papadakis CM. Self-assembled micelles from thermoresponsive poly (methyl methacrylate)-b-poly (N-isopropylacrylamide) diblock copolymers in aqueous solution. *Macromolecules*. 2020;54(1): 384-397.
47. Saylan Y, Denizli A. Supermacroporous composite cryogels in biomedical applications. *Gels*. 2019;5(2): 20.
48. Yazdanpanah G, Jiang Y, Rabiee B, Omid M, Rosenblatt MI, Shokuhfar T, Pan Y, Naba A, Djalilian AR. Fabrication, Rheological, and Compositional Characterization of Thermoresponsive Hydrogel from Cornea. *Tissue Engineering Part C: Methods*. 2021;27(5): 307-321.
49. Vasile C, Pamfil D, Stoleru E, Baican M. New developments in medical applications of hybrid hydrogels containing natural polymers. *Molecules*. 2020;25(7): 1539.
50. Chen G, Tang W, Wang X, Zhao X, Chen C, Zhu Z. Applications of hydrogels with special physical properties in biomedicine. *Polymers*. 2019;11(9): 1420.
51. Musgrave CS, Fang F. Contact lens materials: a materials science perspective. *Materials*. 2019;12(2): 261.
52. Driest PJ, Allijn IE, Dijkstra DJ, Stamatialis D, Grijpma DW. Poly (ethylene glycol)-based poly (urethane isocyanurate) hydrogels for contact lens applications. *Polymer International*. 2020;69(2): 131-139.
53. Zhao H, Liu M, Zhang Y, Yin J, Pei R. Nanocomposite hydrogels for tissue engineering applications. *Nanoscale*. 2020;12(28): 14976-14995.
54. Jiang L, Wang Y, Liu Z, Ma C, Yan H, Xu N, Gang F, Wang X, Zhao L, Sun X. Three-dimensional printing and injectable conductive hydrogels for tissue engineering application. *Tissue Engineering Part B: Reviews*. 2019;25(5): 398-411.
55. Wang Q, Li S, Wang Z, Liu H, Li C. Preparation and characterization of a positive thermoresponsive hydrogel for drug loading and release. *Journal of Applied Polymer Science*. 2009;111(3): 1417-1425.
56. Sun Y, Nan D, Jin H, Qu X. Recent advances of injectable hydrogels for drug delivery and tissue engineering applications. *Polymer Testing*. 2020;81: 106283.
57. Abasalizadeh F, Moghaddam SV, Alizadeh E, Kashani E, Fazljou SM, Torbati M, Akbarzadeh A. Alginate-based hydrogels as drug delivery vehicles in cancer treatment and their applications in wound dressing and 3D bioprinting. *Journal of Biological Engineering*. 2020;14(1): 1-22.

58. Etter M, Dinnebier RE. A century of powder diffraction: a brief history. *Zeitschrift für anorganische und allgemeine Chemie*. 2014;640(15): 3015-3028.
59. Graewert MA, Svergun DI. Impact and progress in small and wide angle X-ray scattering (SAXS and WAXS). *Current Opinion in Structural Biology*. 2013;23(5): 748-754.
60. Varaprasad K, Mohan YM, Ravindra S, Reddy NN, Vimala K, Monika K, Sreedhar B, Raju KM. Hydrogel–silver nanoparticle composites: a new generation of antimicrobials. *Journal of Applied Polymer Science*. 2010;115(2): 1199-1207.
61. Denzer BR, Kulchar RJ, Huang RB, Patterson J. Advanced Methods for the Characterization of Supramolecular Hydrogels. *Gels*. 2021;7(4): 158.

THE AUTHORS

Nidhi Mishra

e-mail: nidhimishra@iiita.ac.in

ORCID: 0000-0002-6028-7723

Akhilesh Kumar Maurya

e-mail: rss2018504@iiita.ac.in

ORCID: 0000-0003-3281-532X

Shagun Varshney

e-mail: shagun3733@gmail.com

ORCID: 0000-0002-3248-5925